Supplementary Information

From understanding the formation mechanism to enhanced supercapacitor performance of VSB-5 with hierarchical structure

Yue Zhang, Rudan Hu, Feng Wen, Jianli Zhang, Yining Wang, Richao Niu, Xin Wang, and Junwu Zhu*.

Key Laboratory for Soft Chemistry and Functional Materials (Nanjing University of Science and Technology), Ministry of Education, Nanjing 210094, China.

**To whom correspondence should be addressed. E-mail: zhujw@njust.edu.cn.*

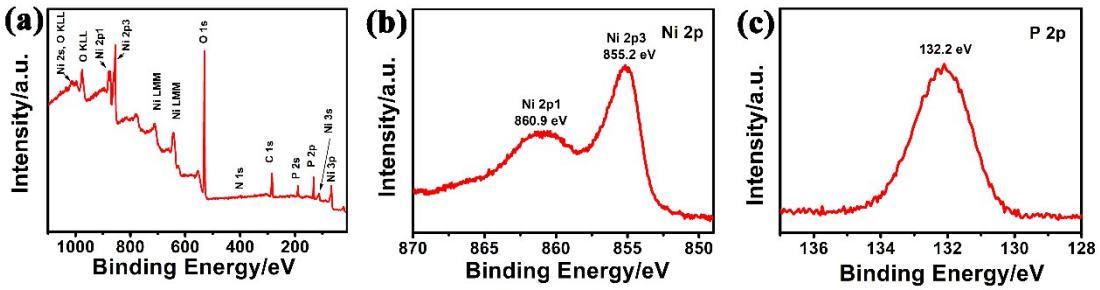

Fig. S1 XPS spectra of $NP_{3.5}$: (a) complete survey, (b) Ni 2p, and (c) p 2p.

As shown in Fig. S1a, the complete survey indicates that Ni, P, O and N elements in $NP_{3.5}$ can be detected. The weak peak of N for NP3.5 may be due to the adsorption of aqueous ammonia. The XPS spectra of Ni 2p and P 2p of $NP_{3.5}$ are shown in Fig. S1b,c.

Table S1 XPS atomic percentage of elements observed on the surface of $NP_{3.5}$.

Element	Ni 2p3	P 2p	O 1s	N 1s
Atomic %	30.7	8.4	59.3	1.6

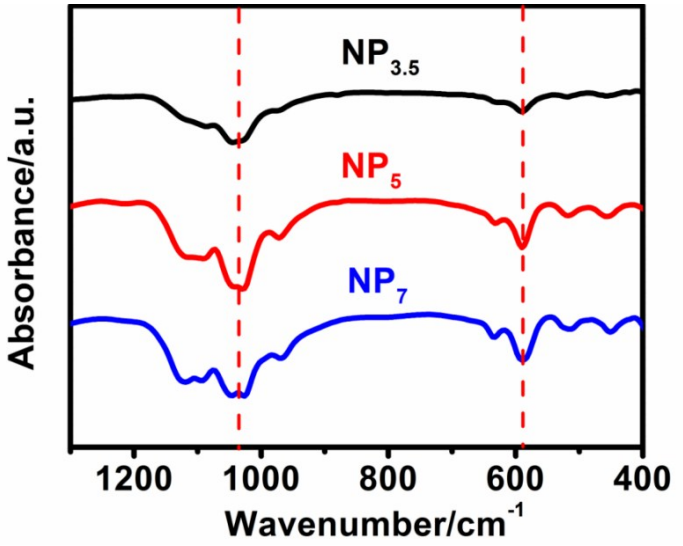

Fig. S2 FTIR spectra of $NP_{3.5}$, NP_5, and NP_7.

In Fig. S2, the FTIR spectra of $NP_{3.5}$, NP_5, and NP_7 have similar absorption bands around 1049 cm^{-1} and 586 cm^{-1} (as indicated by the red dashed lines), and these bonds could be attributed to the presence of PO_4^{3-}. Besides, bonds around 111 cm^{-1}, 1026 cm^{-1}, 968 cm^{-1}, 636 cm^{-1}, 516 cm^{-1} and 455 cm^{-1} can be assigned to HPO_4^{2-}. Since the HPO_4^{2-} is only existence in VSB-5, it can be speculated that all of the three substance contain VSB-5.

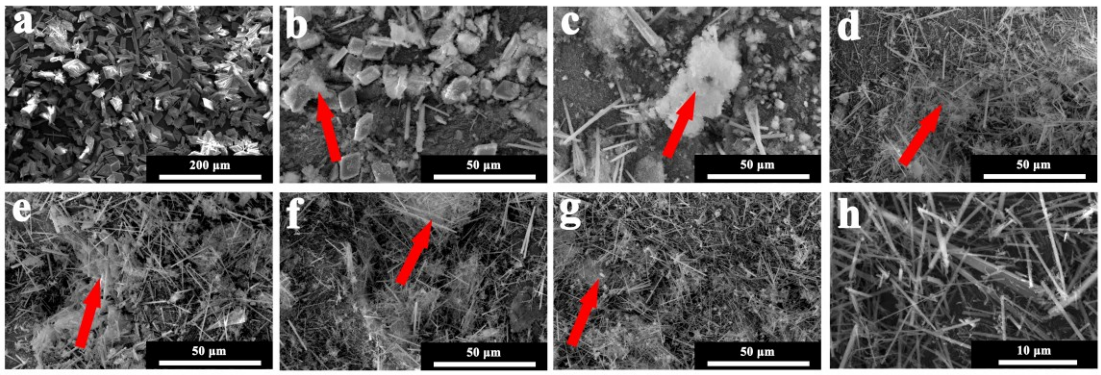

Fig. S3 SEM images of the nickel phosphates obtained with different adding amount aqueous ammonia: (a) 0.4 mL, (b) 0.8 mL, (c) 1 mL, (d) 1.2 mL, (e) 2 mL, (f) 3.5 mL, (g) 5 mL, and (h) 7 mL.

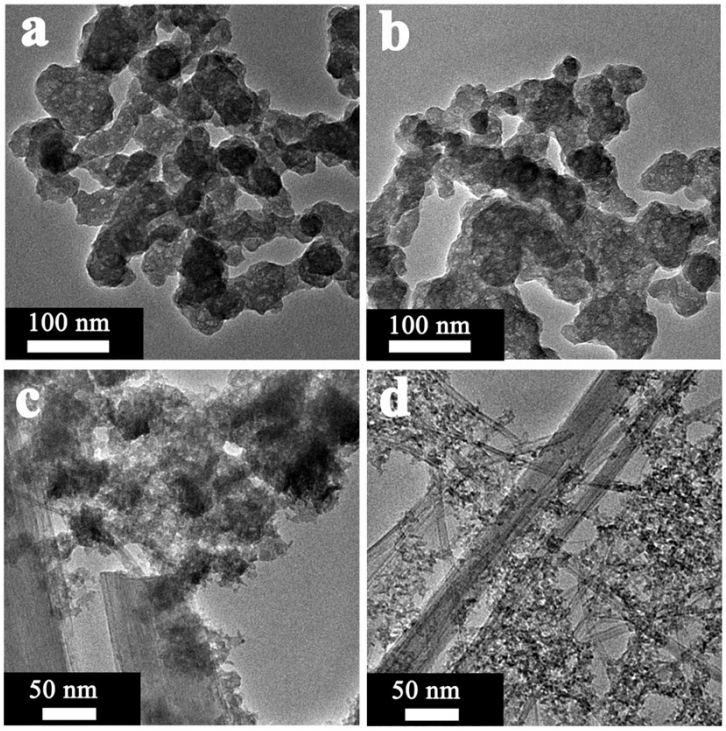

Fig. S4 TEM images of (a) $NP_{0.8}$, (b) NP_1, (c) $NP_{3.5}$, and (d) NP_5. The amorphous part was selected as the main characterization area.

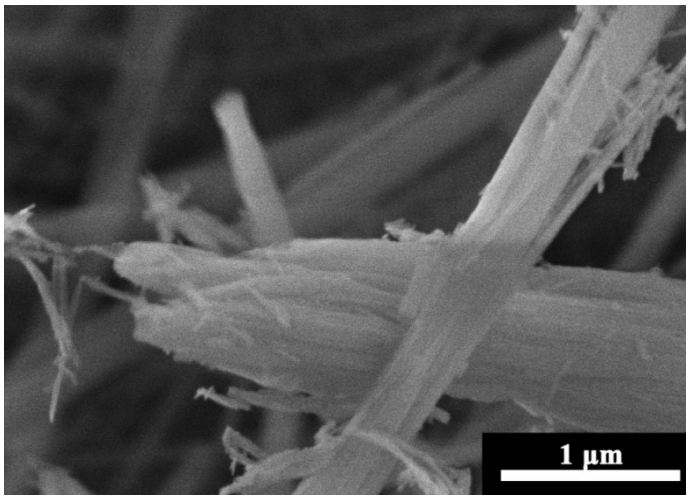

Fig. S5 SEM image of rod-like VSB-5 (NP_7).

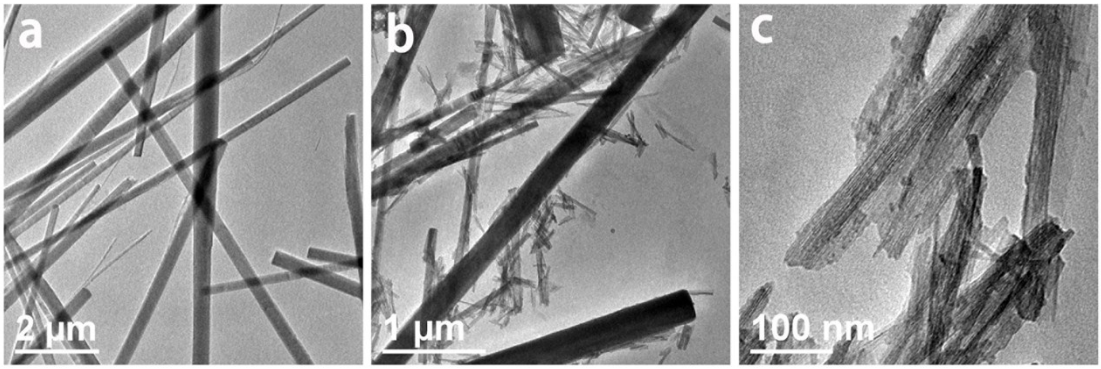

Fig. S6 TEM images of NP_7: (a) before , (b) and (c) after ultrasonication for 5h.

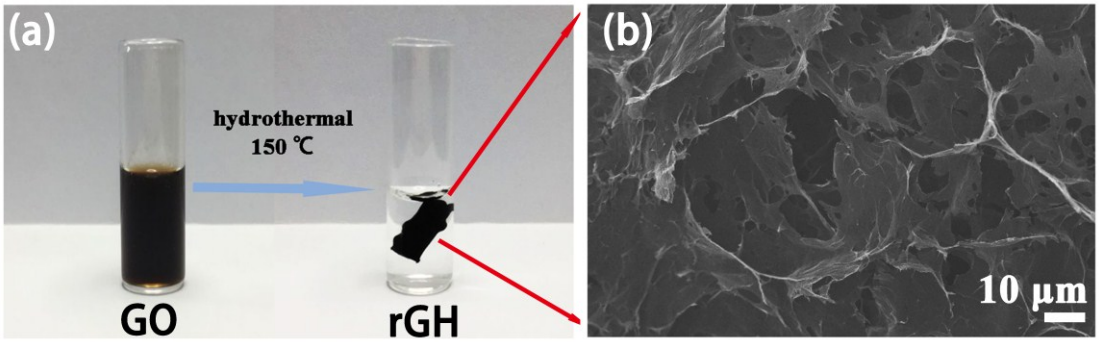

Fig. S7 (a) photograph of GO and rGH. (b) SEM image of 3D rGH.

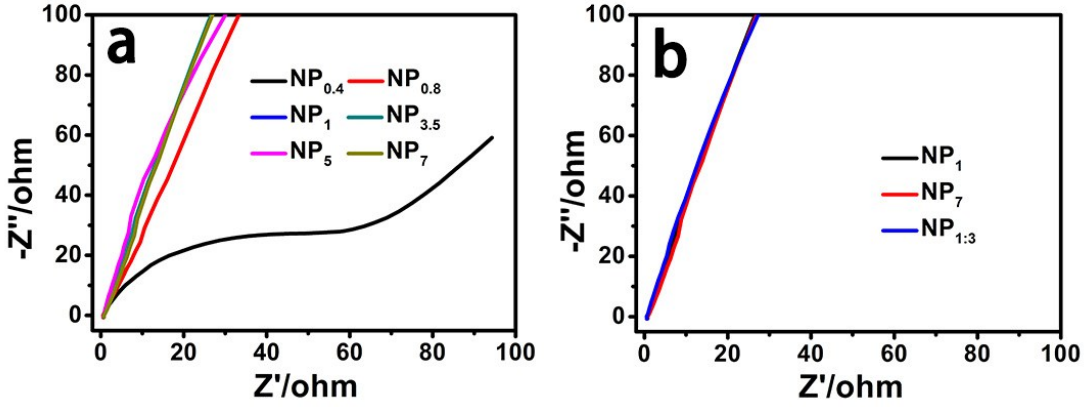

Fig. S8 Nyquist plots of the nickel phosphates: (a) $NP_{0.4}$, $NP_{0.8}$, NP_1, $NP_{3.5}$, NP_5, NP_7, and (b) NP_1, NP_7, $NP_{1:3}$.

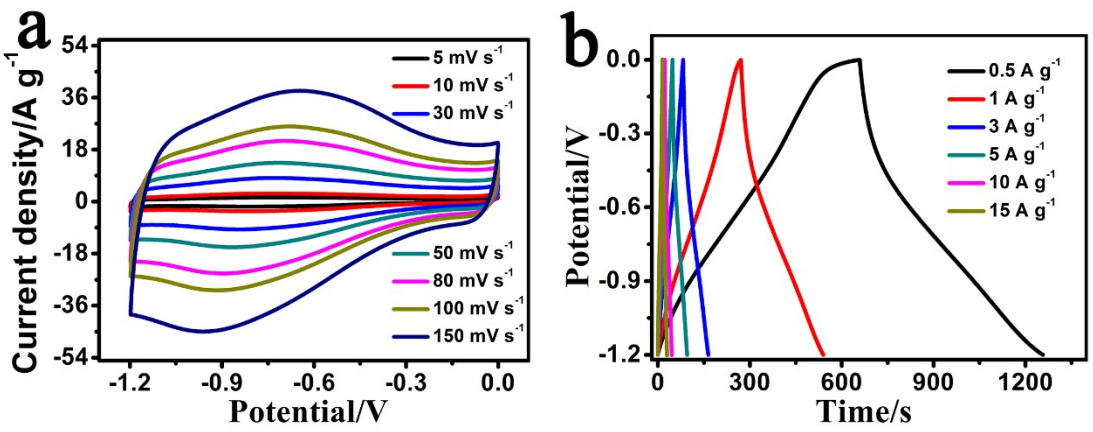

Fig. S9 (a) CV curves and (b) galvanostatic charge-discharge curves of rGH in a three-electrode system with 6 M KOH aqueous.

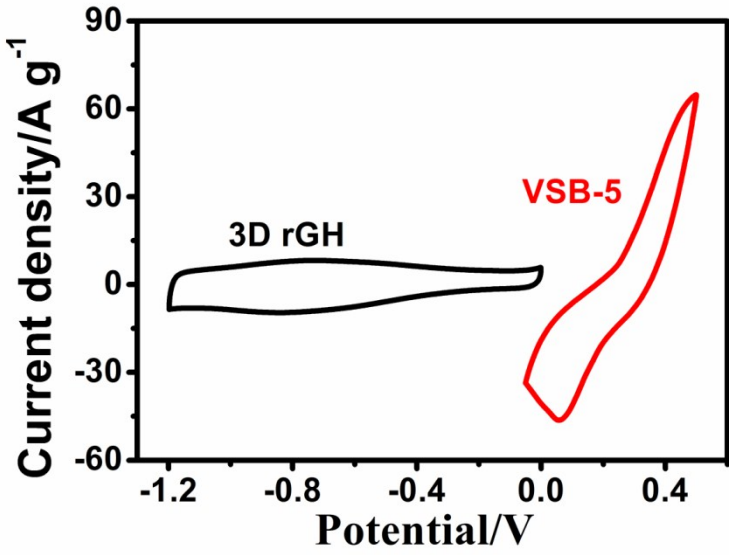

Fig. S10 CV curves of NP_7 and rGH at a scan rate of 30 mV s^{-1} in a three-electrode system with 6 M KOH aqueous.

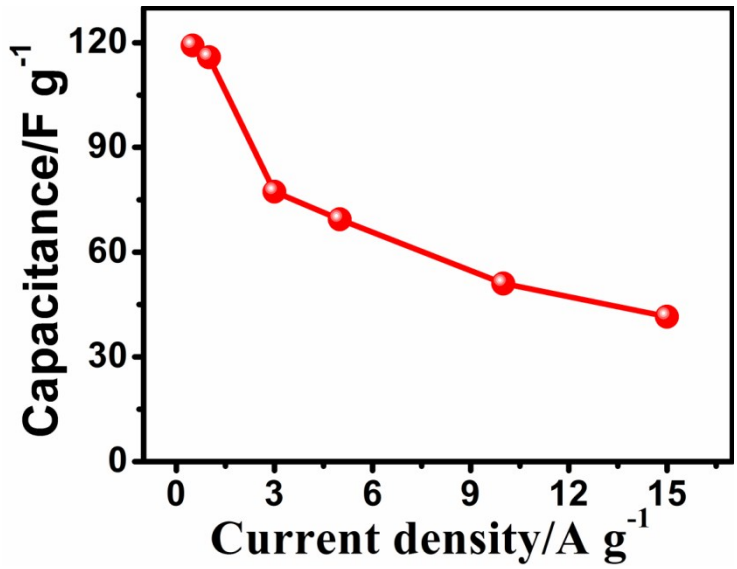

Fig. S11 The rate capability of HSC NP_7//rGH.